Journal of Alloys and Compounds 509 (2011) 1333–1337

Contents lists available at ScienceDirect

Journal of Alloys and Compounds

journal homepage: www.elsevier.com/locate/jallcom

Structural, magnetic and dielectric properties of $La_{2-x}Ca_xNiO_{4+\delta}$ ($x = 0, 0.1, 0.2, 0.3$)

Chen-Yang Shi [a], Zhong-Bo Hu [b], Yong-Mei Hao [a,*]

[a] College of Chemistry and Chemical Engineering, Graduate University of Chinese Academy of Sciences, 19 (A) Yu Quan Road, Beijing, 100049, China
[b] College of Materials and Photoelectric Technology, Graduate University of Chinese Academy of Sciences, 19(A) Yu Quan Road, Beijing, 100049, China

ARTICLE INFO

Article history:
Received 24 August 2010
Received in revised form 1 October 2010
Accepted 7 October 2010
Available online 15 October 2010

Keywords:
Ceramics
Solid state reaction
Crystal structure
Dielectric response
Magnetic measurements

ABSTRACT

The synthesis, structural, magnetic and dielectric properties of a new type of high permittivity materials $La_{2-x}Ca_xNiO_{4+\delta}$ ($x = 0, 0.1, 0.2, 0.3$) (abbreviated as LCNs) were reported. The samples were prepared through conventional solid state reaction route. Detailed structural information was retrieved by Rietveld refinement; normalized bond length and bond valence was calculated to investigate the compression/dilation effect of bonds and atoms in unit cell. It can be found all samples belong to K_2NiF_4 structure with space group $I4/mmm$. Doping of Ca in $La_2NiO_{4+\delta}$ shrinks the unit cell and makes the structure tend to become instable. Three types of (La, Ca)–O bonds, and two kinds of Ni–O bonds exist in LCNs. Along c axis there are alternately compressed (La,Ca)O_9 dodecahedra and lengthened NiO_6 octahedra. Room temperature magnetic measurements show that the materials are paramagnetic and Ca doping can improve the spontaneous magnetization. Furthermore, all samples have colossal values of the dielectric constant (ε) at frequencies lower than 1 kHz. Interestingly, $La_{1.8}Ca_{0.2}NiO_{4+\delta}$ maintains its high permittivity at frequencies up to 1 MHz while $La_{1.7}Ca_{0.3}NiO_{4+\delta}$ has the lowest dielectric loss ($\tan\delta$). Calcium doping can effectively enhance ε and inhibit $\tan\delta$. The distortion of (La,Ca)O_9 dodecahedra can well explain their dielectric properties.

1. Introduction

In recent years, materials with K_2NiF_4 structure have been widely used as solid oxide fuel cells (SOFC) such as $Ba_{1.2}Sr_{0.8}CoO_{4+\delta}$, $LaSrFeO_{4+\delta}$, $Sr_{2-x}La_xMnO_{4+\delta}$ [1–3]. In addition, in the process of searching for new types of giant dielectric constant materials [4–11], modified K_2NiF_4 structured materials also play an important role and exhibit excellent dielectric properties, for instance substituted $CaLaAlO_4$, $CaNdAlO_4$, $SrNdCoO_4$ [12–14]. $La_2NiO_{4+\delta}$ is another member of K_2NiF_4 family and therefore it is meaningful to study the dielectric properties of modified $La_2NiO_{4+\delta}$ system. Some research groups have already studied Sr doped $La_2NiO_{4+\delta}$ [15–17], Ba doped $La_2NiO_{4+\delta}$ [18] and found colossal dielectric behavior. But the origin of giant dielectric constant is still disputable: Park et al. [15] and Liu et al. [16] ascribed the origin to "charge glassiness" or polaron hopping. However, Sachan et al. [17] believed the Maxwell–Wagner relaxation induced by inhomogeneous charge distribution should be responsible.

In $SrRAlO_4$ (R = Sm, La, Nd), Fan et al. [19] tried to explain their dielectric properties by establishing the relationship among structural parameters, polar-phonon modes parameters, and dielectric properties. Similar to Sr, Ca is another promising element that can be used to improve dielectric properties of $La_2NiO_{4+\delta}$ but till now few papers focused on this system. In this study, we investigate the dielectric properties of Ca doped $La_2NiO_{4+\delta}$ and try to explain them by structure–property relationship. Hopefully, our work can provide guidance for finding new colossal dielectric constant materials. Besides, since $La_2NiO_{4+\delta}$ contains magnetic element Ni, it is also worthwhile to study its magnetic property.

2. Experimental

$La_{2-x}Ca_xNiO_{4+\delta}$ ($x = 0, 0.1, 0.2, 0.3$) were fabricated by conventional solid-state reaction method. Analytical-grade raw materials, La_2O_3, $CaCO_3$ and NiO were weighed and mixed in a ball mill for 10 h using alcohol as the milling media. After drying, the powders were pre-sintered at 1000 °C, 1100 °C, and 1200 °C each for 12 h in air and then taken out and remilled for 4 h. Then a final sintering at a temperature 1300 °C continued for another 24 h.

X-ray diffraction was used to determine the crystallographic structure. Room temperature X-ray diffraction (XRD) data were collected on MSAL-XD2 using Cu Kα radiation with a 2θ range from 10° to 90° at a step width of 0.01° at Laboratory of Inorganic Materials of Graduate University of Chinese Academy of Sciences.

Room temperature M-H loop was recorded by MPMS-5 Quantum Design SQUID at Institute of Physics, Chinese Academy of Sciences.

The impedance analyzer (HP4192A) was used to characterize the dielectric properties at room temperature.

3. Results and discussion

3.1. Crystal structure

Fig. 1 shows the powder X-ray diffraction patterns of $La_{2-x}Ca_xNiO_{4+\delta}$ ($x = 0$–0.3) samples and it is evident that no sec-

* Corresponding author. Tel.: +86 10 88256414; fax: +86 10 88256093.
E-mail address: ymhao@gucas.ac.cn (Y.-M. Hao).

0925-8388/$ – see front matter © 2010 Elsevier B.V. All rights reserved.
doi:10.1016/j.jallcom.2010.10.030

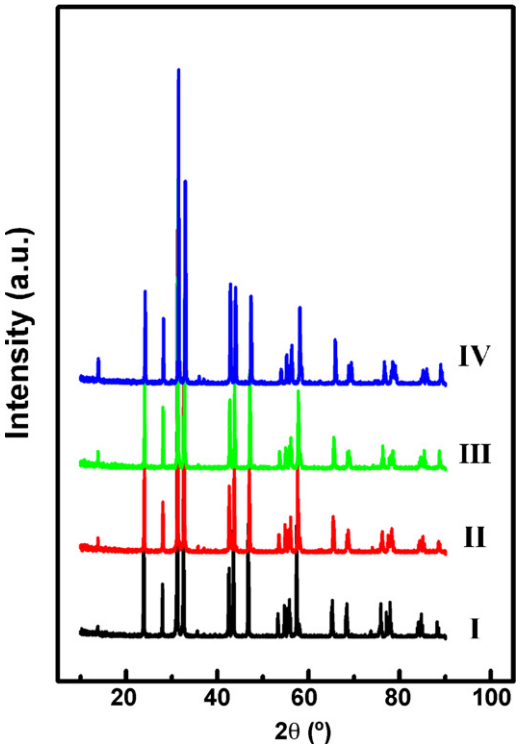

Fig. 1. Room temperature X-ray diffraction patterns of (I → IV) $La_{2-x}Ca_xNiO_{4+\delta}$ with $x = 0, 0.1, 0.2, 0.3$.

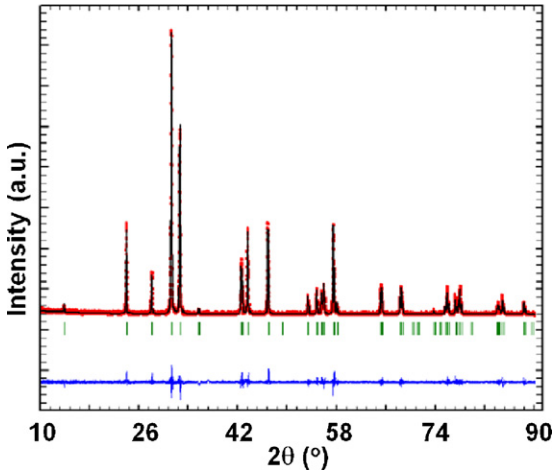

Fig. 2. Rietveld refinement of $La_2NiO_{4+\delta}$: observed (open circles), calculated (continuous line) and difference (continuous line near the bottom) plots after the final cycle of refinement in the *I*4/*mmm* space group. The vertical bars indicate positions of Bragg peaks.

Table 1
Effective ionic radii used in this work for calculation of bond length and bond valence.

	La^{3+}	Ca^{2+}	Ni^{2+}	O^{2-}
Coordination number	9	9	6	6
Shannon radius	1.216 Å	1.18 Å	0.69 Å	1.40 Å

ondary phase appears. Software Fullprof 2009 was used to refine the structure of samples. Besides, two parameters were also used to analyze the stability of LCNs. One is tolerance factor and can be calculated by $t = (r_A + r_O)/[2^{1/2}(r_B + r_O)]$ where r_A, r_O, r_B are the effective radii of La, Ca, O, Ni [20] and listed in Table 1. The other one is Global instability index (*GII*) and can be obtained by the following equations: $GII = [\sum d_i^2/i]^{1/2}$, $d_i = V_i - \sum S_{ij}$, $S_{ij} = \exp[(D_0 - D_{ij})/B]$, where D_{ij} and S_{ij} are bond length and bond valence respectively, B is a constant 0.37, D_0 is the bond length of unit valence. Formal valence of ion and the deviation valence are described as V_i and d_i [21–25]. Tolerance factor reflects the stability of structure and the structure is stable if t is close to 1. For a K_2NiF_4-type structure, the t value somewhat indicates the size adaptability between perovskite and rocksalt layers. While *GII* represents the instability of the structure and a larger *GII* indicates a less stable structure. Fig. 2 displays the Rietveld refinement of $La_2NiO_{4+\delta}$ and the refined structural parameters are summarized in Table 2.

Table 2
Structural parameters of $La_{2-x}Ca_xNiO_{4+\delta}$ ($x = 0, 0.1, 0.2, 0.3$) samples[a].

Compounds	$La_2NiO_{4+\delta}$	$La_{1.9}Ca_{0.1}NiO_{4+\delta}$	$La_{1.8}Ca_{0.2}NiO_{4+\delta}$	$La_{1.7}Ca_{0.3}NiO_{4+\delta}$
Crystal system	Tetragonal			
Space group	*I*4/*mmm* (139)			
Lattice parameters				
a (Å)	3.868(5)	3.853(9)	3.844(1)	3.825(5)
c (Å)	12.684(5)	12.654(9)	12.635(6)	12.604(2)
c/*a*	3.278(9)	3.283(7)	3.287(0)	3.294(8)
Cell volume (Å^3)	189.815(6)	187.954(7)	186.720(6)	184.457(6)
La/Ca				
z	0.3607(4)	0.3610(7)	0.3617(7)	0.3616(3)
O_2				
z	0.1781(8)	0.1778(5)	0.1780(6)	0.1743(2)
R factors				
R_{wp}	0.139	0.141	0.148	0.143
R_p	0.101	0.104	0.112	0.104
R_B	0.0515	0.0484	0.0665	0.0473
Bond length (Å)				
Ni–O(1) (Å)	1.934(3)	1.927(0)	1.922(1)	1.912(8)
Ni–O(2) (Å)	2.260(1)	2.250(7)	2.249(9)	2.197(1)
(La Ca)–O(1) (Å)	2.619(5)	2.608(5)	2.597(1)	2.588(5)
(La Ca)–O(2a) (Å)	2.779(7)	2.769(3)	2.764(4)	2.742(7)
(La Ca)–O(2b) (Å)	2.315(7)	2.318(6)	2.321(3)	2.360(9)
Tolerance factor	0.8852	0.8846	0.8840	0.8834
GII	0.2904	0.3162	0.3595	0.4952

[a] Atomic fractional coordinate of (La, Ca) and O(2) are (0, 0, *z*), those of Ni and O(1) are (0,0,0) and (0, 1/2, 0) respectively.

According to Table 2, one can conclude, first, all samples crystallize in tetragonal structure with space group *I*4/*mmm*, indicating a typical K_2NiF_4 structure. Second, Ca has successfully replaced La and entered the lattice because the lattice parameters *a*, *b*, *c* and *V* decrease monotonously with increasing amount of Ca. The shrinkage of cell is due to the substitution of smaller Ca^{2+} (1.18 Å) for larger La^{3+} (1.216 Å). Finally, combining the variation of tolerance factors and *GII*, doping of Ca makes the structure become unstable.

3.2. Bond length and bond valence

Normalized bond length can be utilized to analyze compression/dilation effects of cation–oxygen bonds. It is the ratio of the calculated bond length (actual bond length) to the sum of effective ionic radii (theoretical bond length) [20] listed in Table 1. If this ratio is larger than 1, the cation–oxygen bond is elongated, otherwise, compressed. By comparison, normalized bond valence of any bond and bond valence sum (BVS) of any atom in LCNs can be obtained by dividing ideal bond valence of each cation–oxygen bond and ideal valence of any atom into calculated ones respectively. Contrary to normalized bond length, any bond with a normalized bond valence value larger than 1 is shortened otherwise lengthened; any atom with a normalized bond valence sum value larger than 1 is compressed otherwise elongated. Fig. 3(a)–(c) depicts the variation of normalized bond length, bond valence and bond valence sum. In order to better understand these, a ball and stick model is given in Fig. 4.

From Fig. 3, one can know that there are three types of (La, Ca)–O bonds, and two kinds of Ni–O bonds in LCNs. Among these bonds, (La, Ca)–O(2b) and Ni–O(1) bonds are compressed while (La,Ca)–O(2a) bonds and Ni–O(2) bonds are elongated. In contrast, the calculated normalized values of (La, Ca)–O(1) bonds vibrate around 1, suggesting little stress or rattling effect in these bonds. Regarding atoms, O1, Ni are compressed while Ca, O2 are lengthened. Atom La is rattling.

Ball and stick model is displayed in Fig. 4, one may find along *c* axis there are alternately (La, Ca)O_9 dodecahedra and NiO_6 octahedra. Along *c* axis, in (La,Ca)O_9, (La,Ca)–O(1) have little stress while (La,Ca)–O2(b) are compressed, thus the dodecahedra is compressed; as for NiO_6, because Ni–O(2) bonds are elongated thus the octahedra is lengthened. The compression of dodecahedra and elongation of octadedra along *c* axis achieve a zero-change in lattice parameter *c*.

3.3. Room temperature magnetic properties

The *M*–*H* curves measured at room temperature in an applied magnetic field up to 5 T are shown in Fig. 5, one may find that the magnetic moment induced by the high applied field is linear in the field strength and rather weak. Thus it indicates that all the LCNs exhibit paramagnetic behavior. In addition, doping of Ca leads to an enhanced spontaneous magnetization. In a similar compound $BiFeO_3$, substitution of Bi by divalent Ca, Sr, Pb, Cd ions could result in an enhanced spontaneous magnetization too [26–29]. It is explained that first, structural disorder brought by doping could cause canting of Fe spins and in most cases it is accompanied by the decrease of tolerance factor [29]. Second, replacement of Bi with an isovalent cation (+2) could lead to either appearance of Fe^{4+} (forming Fe^{3+}–O–Fe^{4+} double exchange interaction) or oxygen vacancies [30,31]. Similarly, in the case of Ca doped $La_2NiO_{4+\delta}$, as Ca increases, one may find tolerance factor decreases from 0.8852 to 0.8834 and *GII* increases from 0.2904 to 0.4952, which indicate a larger structural disorder. The canting of Ni spins might be responsible for the improved magnetization. In addition, Ni^{2+}–O–Ni^{3+} double exchange interaction might also play some active role, which is in accordance with the result from Klingeler et al. [32]. Being different

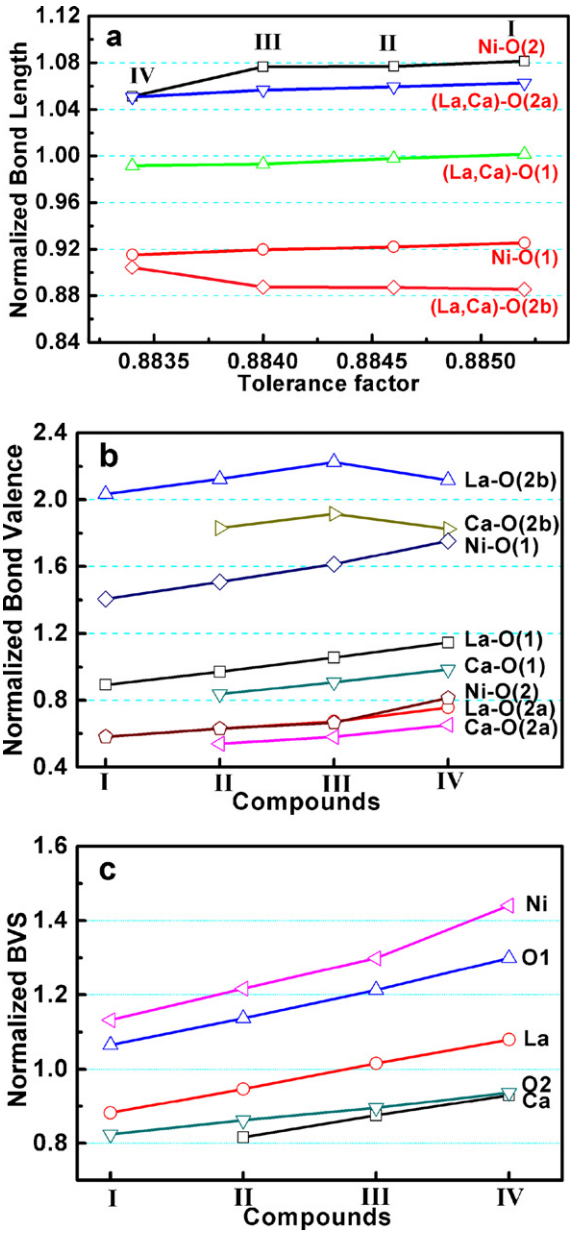

Fig. 3. (a) Compression and dilation effects of selected bonds in (I → IV) $La_{2-x}Ca_xNiO_{4+\delta}$ (x = 0, 0.1, 0.2, 0.3) as a function of tolerance factor. (b) Normalized bond valence of each bond in (I → IV) $La_{2-x}Ca_xNiO_{4+\delta}$ with x = 0, 0.1, 0.2, 0.3. (c) Normalized bond valence sum of each ion in (I → IV) $La_{2-x}Ca_xNiO_{4+\delta}$ with x = 0, 0.1, 0.2, 0.3.

from $BiFeO_3$, oxygen vacancy may be not the reason in this study. Poirot et al. [33] confirmed the amount of oxygen concentration in $La_{2-x}Ca_xNiO_{4+\delta}$ ($x < 0.5$) by thermo-gravimetric analysis and found out even for $x = 1/3$, δ is still larger than zero. Besides, Ruck et al. [34] pointed out if the $La_{2-x}Ca_xNiO_{4+\delta}$ system is tetragonal with space group *I*4/*mmm*, it has excessive amount of oxygen. More details about oxygen transport in $La_2NiO_{4+\delta}$ can refer to a review by Chroneos et al. [35]. In current system oxygen stay in interstitial sites and the excessive oxygen concentration (hole content) influences the magnetization. The hole concentration, defined as $n_H = x + 2\delta$ for $La_{2-x}Ca_xNiO_{4+\delta}$, increases with the increasing amount of calcium [33]. More holes insert into Ni-sites, leading to an increasing number of Ni^{3+}. Ni^{3+} can interact with Ni^{2+}, thus achieves larger magnetization.

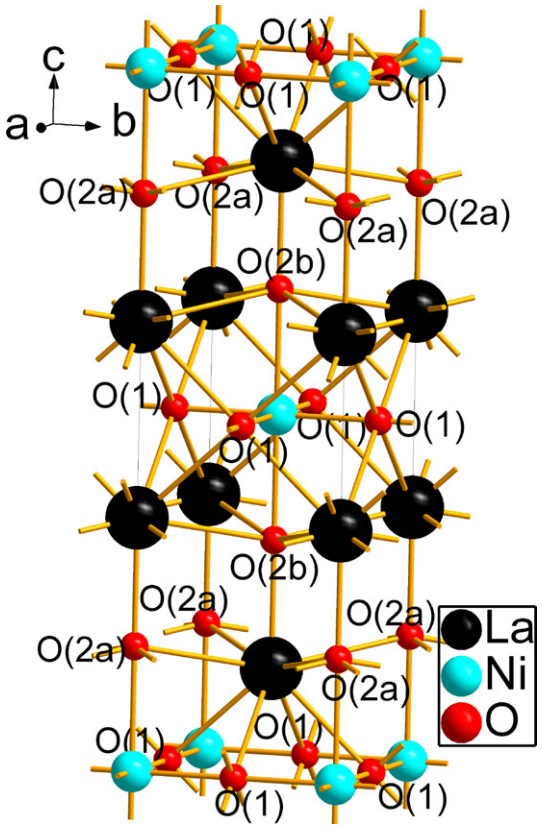

Fig. 4. Ball and stick model for LCNs. Ni and O atoms are represented by cyan and red, Ca or La by black.

3.4. Room temperature dielectric properties

As presented in Fig. 6(a), all prepared LCNs exhibit colossal dielectric constant (ε) at frequencies lower than 1 kHz. For example, at 100 Hz, the ε values for $La_{2-x}Ca_xNiO_{4+\delta}$ ($x = 0$, 0.1, 0.2, 0.3) are 7.86×10^4, 6.51×10^4, 4.78×10^5, 1.49×10^5 respectively. However, when applied frequency increases to 1 kHz these values decrease dramatically to 553.1, 2980, 5790, 11500 and at 1 MHz the corresponding dielectric constants are 201.7, 46.1, 5103 and 37.9. Interestingly, it is found that $La_{1.8}Ca_{0.2}NiO_{4+\delta}$ maintains its high permittivity up to a comparatively higher frequency (around 1 MHz) (see inset), which might be influenced by the extrinsic behavior of the material and further experiment is needed. Similar result was also reported by Krohns et al. [36] and they

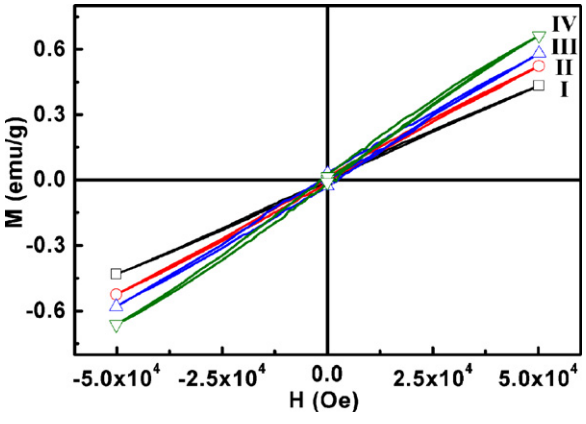

Fig. 5. Magnetic hysteresis loops of (I → IV) $La_{2-x}Ca_xNiO_{4+\delta}$ with $x = 0$, 0.1, 0.2, 0.3 measured at room temperature in an applied magnetic field up to 5 T.

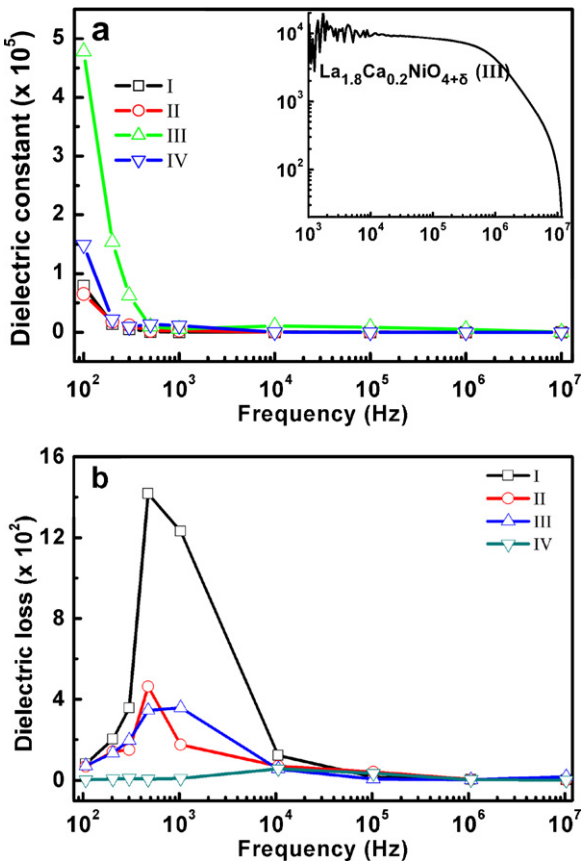

Fig. 6. (a) Room temperature dielectric constant of (I → IV) $La_{2-x}Ca_xNiO_{4+\delta}$ ($x = 0$, 0.1, 0.2, 0.3) as a function of frequency (100 Hz-10 MHz). Inset: frequency dependent permittivity of $La_{1.8}Ca_{0.2}NiO_{4+\delta}$ (1 kHz–10 MHz). (b) Room temperature dielectric loss of (I → IV) $La_{2-x}Ca_xNiO_{4+\delta}$ ($x = 0$, 0.1, 0.2, 0.3) as a function of frequency (100 Hz–10 MHz).

claimed that a charge-ordered nickelate $La_{15/8}Sr_{1/8}NiO_4$ retains its colossal magnitude larger than 10^4 into the GHz range. And they hold that the reason for enhanced dielectric constant is possibly charge-order due to inhomogeneous charge distribution. From a structure–property point of view, distortion of $(La,Ca)O_9$ dodecahedra should also be responsible for unusual dielectric constant and to be specific, (La,Ca)–O(2a), (La,Ca)–O(2b) and (La,Ca)–O(1) bonds influence the dielectric constant [19]. As indicated in Fig. 3(a), from $La_2NiO_{4+\delta}$ to $La_{1.7}Ca_{0.3}NiO_{4+\delta}$, (La,Ca)–O(1) has little change, thus has no contribution to dielectric constant. However, the compression of (La,Ca)–O(2b) is released to some extent and (La,Ca)–O(2a) are always elongated. The elongation of these two bonds may contribute to the enhancement of dielectric constant.

In Fig. 6(b), it can be found that all samples have experienced dielectric relaxation process featured by the peaks appeared. These peaks correspond to Maxwell–Wagner type relaxation. Besides, doping of Ca can effectively inhibit dielectric loss. Fan et al. [19] try to explain the dielectric loss from the relationship between two polar-phonon modes and structure. According to their theory, dielectric loss is influenced by (La,Ca)–O(1), (La,Ca)–O(2a) and (La,Ca)–O(2b) bonds and if the normalized values of any cation–oxygen bond approach 1, it will reduce the dielectric loss. In this study (Fig. 3(b)), from $La_2NiO_{4+\delta}$ to $La_{1.7}Ca_{0.3}NiO_{4+\delta}$, normalized bond valences of Ca–O(1), Ca–O(2a) and La–O(2a) approach 1, which reduces the dielectric loss greatly. As for La–O(2b) and Ca–O(2b), because they are heavily compressed, they only increase the loss. The minimum elongation of Ca–O(1), Ca–O(2a) and La–O(2a) bonds explains $La_{1.7}Ca_{0.3}NiO_{4+\delta}$ has the lowest loss among all prepared materials. However, it is worth noting that

structural parameters can only explain the intrinsic part of dielectric properties. In reality extrinsic factors such as porosity, grain boundary should also be taken into consideration. Besides, having in mind that even for much investigated $CaCu_3Ti_4O_{12}$ (CCTO) no consensus has been achieved so far [37,38], many efforts should also be made for further clarification.

4. Conclusions

$La_{2-x}Ca_xNiO_{4+\delta}$ (x = 0, 0.1, 0.2, 0.3) ceramics were obtained through traditional solid state reaction method. Rietveld refinement results suggest all samples crystallize in K_2NiF_4 structure with space group $I4/mmm$. LCNs exhibit paramagnetic response and addition of Ca leads to an improved spontaneous magnetization. LCNs show colossal dielectric constant at low frequency. Among all samples, $La_{1.8}Ca_{0.2}NiO_{4+\delta}$ maintains its high permittivity up to 1 MHz while $La_{1.7}Ca_{0.3}NiO_{4+\delta}$ has the lowest loss. Doping of Ca can effectively enhance ε and inhibit tan δ. Through the calculated bond length and valence, it is known along c axis (La,Ca)O_9 dodecahedra is compressed while NiO_6 octahedra is lengthened. Change of (La,Ca)–O(2b), (La,Ca)–O(2a) together with (La,Ca)–O(1) within (La,Ca)O_9 dodecahedra play a role in enhancement of dielectric properties of LCNs.

Acknowledgement

This work was supported by the National Basic Research Program of China (973 Program) 2006CB705601, the President Fund of GUCAS.

References

[1] C. Jin, J. Liu, J. Alloys Compd. 474 (2009) 573–577.
[2] J.H. Huang, X.Y. Jiang, X.B. Li, A.Q. Liu, J. Electroceram. 23 (2009) 67–71.
[3] L.P. Sun, L.H. Huo, H. Zhao, Q. Li, C. Pijolat, J. Power Sources 179 (2008) 96–100.
[4] C.H. Mu, P. Liu, Y. He, J.P. Zhou, H.W. Zhang, J. Alloys Compd. 471 (2009) 137–141.
[5] J.B. Wu, C.W. Nan, Y.H. Lin, Y. Deng, Phys. Rev. Lett. 89 (2002) 217601.
[6] A.A. Dakhel, J. Alloys Compd. 488 (2009) 31–34.
[7] I.P. Raevski, S.A. Prosandeev, A.S. Bogatin, M.A. Malitskaya, L. Jastrabik, J. Appl. Phys. 93 (2003) 4130–4136.
[8] Z. Wang, X.M. Chen, L. Ni, X.Q. Liu, Appl. Phys. Lett. 90 (2007) 022904.
[9] Y.Y. Liu, X.M. Chen, X.Q. Liu, L. Li, Appl. Phys. Lett. 90 (2007) 122905.
[10] H.X. Yuan, X.M. Chen, M.M. Mao, J. Am. Ceram. Soc. 92 (2009) 2286–2290.
[11] Y.Y. Liu, X.M. Chen, X.Q. Liu, L. Li, J. Electroceram. 21 (2008) 706–710.
[12] Y. Xiao, X.M. Chen, X.Q. Liu, J. Electroceram. 21 (2008) 154–159.
[13] C.C. Homes, T. Vogt, S.M. Shapiro, S. Wakimoto, A.P. Ramirez, Science 293 (2001) 673–676.
[14] L. Ni, X.M. Chen, Appl. Phys. Lett. 91 (2007) 122905.
[15] T. Park, Z. Nussinov, K.R.A. Hazzard, V.A. Sidorov, A.V. Balatsky, J.L. Sarrao, S.W. Cheong, M.F. Hundley, J.S. Lee, Q.X. Jia, J.D. Thompson, Phys. Rev. Lett. 94 (2005) 017002.
[16] X.Q. Liu, S.Y. Wu, X.M. Chen, H.Y. Zhu, J. Appl. Phys. 104 (2008) 054114.
[17] V. Sachan, D.J. Buttrey, J.M. Tranquada, J.E. Lorenzo, G. Shirane, Phys. Rev. B 51 (1995) 12742.
[18] C.L. Song, Y.J. Wu, X.Q. Liu, X.M. Chen, J. Alloys Compd. 490 (2010) 605–608.
[19] X.C. Fan, X.M. Chen, X.Q. Liu, Chem. Mater. 20 (2008) 4092–4098.
[20] R.D. Shannon, Acta Cryst. A 32 (1976) 751–767.
[21] A.S. Salinas, J.L.G. Munoz, J.R. Carvajal, R.S. Puche, J.L. Martinez, J. Solid State Chem. 100 (1992) 201.
[22] I.D. Brown, Acta Crystallgr. B 48 (1992) 553.
[23] I.D. Brown, D. Altermatt, Acta Crystallogr., Sect. B 41 (1985) 244.
[24] N.E. Brese, M. O'Keeffe, Acta Crystallogr., Sect. B 47 (1991) 192.
[25] G.H. Rao, K. Baerner, I.D. Brown, J. Phys.: Condens. Matter 10 (1998) L757.
[26] Y.H. Lin, Q. Jiang, Y. Wang, C.W. Nan, L. Chen, J. Yu, Appl. Phys. Lett. 90 (2007) 172507.
[27] D. Lee, M.G. Kim, S. Ryu, H.M. Jang, S.G. Lee, Appl. Phys. Lett. 86 (2005) 222903.
[28] G.L. Yuan, S.W. Or, J. Appl. Phys. 100 (2006) 024109.
[29] D.H. Wang, W.C. Goh, M. Ning, C.K. Ong, Appl. Phys. Lett. 88 (2006) 212907.
[30] T. Matsui, H. Tanaka, N. Fujimura, T. Ito, H. Mabuchi, K. Morii, Appl. Phys. Lett. 81 (2002) 2764.
[31] M.M. Kumar, S. Srinath, G.S. Kumar, S.V. Suryanarayana, J. Magn. Magn. Mater. 188 (1998) 203.
[32] R. Klingeler, B. Buechner, S.–W. Cheong, M. Huecker, Phys. Rev. B 72 (2005) 104424.
[33] N. Poirot, M. Zaghrioui, Solid State Sci. 8 (2006) 149–154.
[34] K. Ruck, G. Krabbes, I. Vogel, Mater. Res. Bull. 34 (1999) 1689–1697.
[35] A. Chroneos, R.V. Vovk, I.L. Goulatis, L.I. Goulatis, J. Alloys Compd. 494 (2010) 190–195.
[36] S. Krohns, P. Lunkenheimer, C. Kant, A.V. Pronin, H.B. Brom, A.A. Nugroho, M. Diantoro, A. Loidl, Appl. Phys. Lett. 94 (2009) 122903.
[37] P. Lunkenheimer, S. Krohns, S. Riegg, S.G. Ebbinghaus, A. Reller, A. Loidl, Eur. Phys. J. Special Topics 180 (2009) 61–89.
[38] M.C. Ferrarelli, D.C. Sinclair, A.R. West, H.A. Dabkowska, A. Dabkowski, G.M. Luke, J. Mater. Chem. 19 (2009) 5916–5919.